Energy-Efficient Resource Allocation for UAV-Enabled Wireless Powered Communications

Saif Najmeddin*§, Ali Bayat§, Sonia Aïssa§, Sofiène Tahar*
*Electrical and Computer Engineering, Concordia University, Montreal, QC, Canada
§INRS-EMT, University of Quebec, Montreal, QC, Canada
Email: {s_najmed, tahar}@ece.concordia.ca, {ali.bayat, sonia.aissa}@emt.inrs.ca

***Abstract*—This paper investigates the energy efficiency optimization in a wireless communication network where devices are wirelessly powered via unmanned aerial vehicle (UAV) to enable uplink data transmission. First, the path loss of the air-to-ground channels is minimized by optimizing the position of the UAV depending on the ground nodes' service demands. Then, using the optimized positioning and a closed-form expression for the energy efficiency, a resource allocation aiming at maximizing the energy efficiency is developed. To this end, two algorithms are proposed, using Lagrangian optimization and gradient decent methods. Numerical results and comparisons are provided. In particular, the results show an enhancement in energy efficiency and reduced wireless power charging time when the ground nodes' demands are taken into consideration.**

***Index Terms*—Energy Harvesting, Energy Efficiency; MIMO; Wireless Power Transfer; Unmanned Aerial Vehicle (UAV).**

I. Introduction

Unmanned aerial vehicles (UAVs), with their high agility and affordable cost, have been receiving significant attention for many applications, including weather forecasting, traffic control, cargo transport, site fire detection, emergency and rescue situations, and communication systems [1]. Recent reports from the federal aviation administration (FAA) show that the number of UAVs will be increasing rapidly in the coming years [2].

Among the wide range of applications enabled by UAVs, their use for achieving high-speed communications is predicted to be an essential part in wireless systems of the future. Along with massive multiple-input multiple-output (MIMO), millimeter wave (mmWave) communications, and energy harvesting, it is expected that the use of UAVs will be one of the most important concepts for the upcoming 5G and beyond, where high data rates shall be provided with better reliability, lower latency, and decreased power consumption compared to the state-of-the-art [3]. Many big corporations started testing UAVs in their platforms. For instance, the possibility of deploying UAVs for Internet connectivity in remote areas has been investigated by Facebook and Google [4]. Also, Qualcomm is exploring the integration of UAVs in current LTE and future 5G cellular applications [5].

Although the deployment of UAVs in communication networks is promising, it comes with a lot of design challenges and reliability problems. For instance, since different network topologies can result due to the mobility of UAVs, effective coordination schemes should be in place to ensure reliability of the network connections, and new communication protocols should be designed accordingly [5]. Also, one of the most critical challenges is the management of the limited on-board energy resources. The energy consumption of the UAV mainly originates from two parts: the transmit/receive platform, and the hardware and mobility [6]. Due to their adjustable altitude and mobility, efficient line-of-sight (LoS) between UAVs and ground nodes (GNs) could be established, thus mitigating signal blockage and shadowing. By this feature, UAVs promise to be an efficient solution to charge battery-limited or hard-to-reach devices through radio frequency (RF) wireless power transfer (WPT) [7].

Several works focus on the resource allocation to enhance the performance of UAV-assisted networks. For instance, optimization of the throughput for a relay-based UAV system is considered in [8] by jointly controlling the UAV trajectory and the source/relay transmit powers. The work in [7] suggests a design based on optimization of the UAVs trajectory to enhance throughput while taking into consideration the energy consumption of the UAV which tries to maximize the amount of energy transferred to GNs during a finite charging period. A placement algorithm is suggested in [9] to efficiently use the UAV transmit power and maximize the coverage of GNs. Throughput maximization of UAV-powered device-to-device communication is investigated in [10], by jointly optimizing the time and power assuring the energy causality constraint on the transmitter side.

Most of the aforementioned works considered single-antenna UAV in their models. Moreover, the details of the air-to-ground channels were not taken into account in most of them. To efficiently use the UAV as a WPT source to charge GNs, a precise resource allocation management has to be conducted to meet the requirements of the energy-limited GNs.

In this work, we address the optimization of the energy efficiency of a system where a multiple-antenna UAV powers GNs via RF WPT, and the energy harvested by the GNs is used for their communication with a terrestrial base station (BS) equipped with a massive antenna array. Within a time slot, the energy harvesting and the information transmission are not conducted at the same time [11]. Accordingly, a time allocation scheme should be in place to specify the optimal timing for switching between the two operations. Moreover, the quality-of-service of the GNs should be guaranteed. Taking into account the said constraints, optimization of the position of the UAV is conducted according to the demands of the GNs, by minimizing the path loss. Afterwards, maximization of the energy efficiency of the communication system is done

978-1-5386-7646-2/19/$31.00 ©2019 IEEE

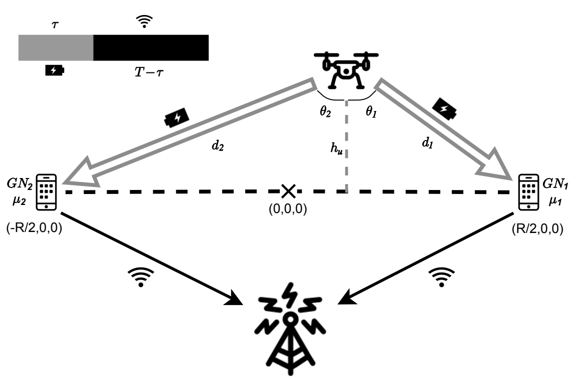

Fig. 1. System Model.

by optimizing the transmit powers towards the GNs and their corresponding wireless power charging time.

The sequel of the paper is organized as follows. Section II details the system model. The optimization problem is formulated and solved in Section III. Numerical results are presented in Section IV. Finally, Section V concludes the paper.

II. System Model

The hovering UAV, equipped with N_u antennas, transmits power wirelessly to GNs during a duration τ which is repeated every time slot T. For simplicity, the 2-user case is considered in this work. From a time slot to the other, the position of the UAV can vary according to the demands of the GNs. Within a time slot, each GN harvests energy from the UAV during time τ, and by applying the *harvest-then-transmit* protocol consumes the harvested energy to transmit its always-available data to the BS during the remaining slot time of $T-\tau$, according to a TDMA-based orthogonal multiple access (OMA) scheme, as shown in Fig. 1. The BS is equipped with a massive antenna array of N_b elements, and its position is denoted (X_b, Y_b, h_b). Without loss of generality, the positions of the GNs are set to $(X_1, Y_1, h_1) = (\mathrm{R}/2, 0, 0)$ and $(X_2, Y_2, h_2) = (-\mathrm{R}/2, 0, 0)$, as shown in Fig. 1. d_1 and d_2 are the distances between the UAV and each GN, respectively. A quantized level of minimum required rate on the uplink is sent from the GN to the UAV to indicate its power demand. Based on this side information, the UAV determines the relative demand of each GN, denoted μ_j, such that $\sum_j \mu_j = 1$. Here, if GN_j has a larger value of μ_j, then it has a higher rate demand which means a higher priority in the WPT.

Let $\mathbf{h}_j$ and $\mathbf{g}_j$, $j = 1, 2$, be the complex channel vectors corresponding to the UAV-GN_j and GN_j-BS links, respectively. $\mathbf{h}_j$ is a row vector and $\mathbf{g}_j$ is a column vector.

On the UAV side, we have $\mathbf{h}_j = \mathbf{h}'_j/\sqrt{L_{d,j}}$, where $L_{d,j}$ and $\mathbf{h}'_j = [h'_{j,1}, h'_{j,2}, \ldots, h'_{j,N_u}]$ denote the average path-loss and the normalized channel fading vector corresponding to UAV-GN_j link, respectively. For the case of Rician fading, the normalized channel vector $\mathbf{h}'_j$ can be written as [12]

$$\begin{aligned}\mathbf{h}'_j &= \mathbf{h}_{LoS,\,j} + \mathbf{h}_{NLoS,\,j} \\ &= \sqrt{\frac{K}{K+1}}\mathbf{1}_{1\times N_u} + \sqrt{\frac{1}{K+1}}\mathbf{h}_{w,j},\end{aligned} \tag{1}$$

where K denotes the Rice factor, $\mathbf{1}_{1\times N_u}$ denotes a unity row vector, $\mathbf{h}_{w,j}$ is a row vector whose elements are independent and identically distributed (i.i.d.) complex Gaussian random variables with zero mean and unit variance; and it is assumed that the UAV antennas are sufficiently apart for the no spatial correlation assumption to hold in defining $\mathbf{h}_{NLoS,j}$'s [13]. Further, the average air-to-ground (A2G) free-space distance-dependent path loss of GNs, $L_{bd,j}$ in dB, is obtained as follows [6]:

$$L_{d,j} = p_{LoS,\,j}\, L_{LoS,\,j} + (1 - p_{LoS,\,j})\, L_{NLoS,\,j}, \tag{2}$$

where the LoS and NLoS path losses are given by

$$L_{LoS,\,j} = 10\; n\; \log_{10}\left(\frac{4\pi f d_j}{c}\right) + \xi_{LoS,\,j}, \tag{3}$$

$$L_{NLoS,\,j} = 10\; n\; \log_{10}\left(\frac{4\pi f d_j}{c}\right) + \xi_{NLoS,\,j}, \tag{4}$$

where n denotes the path loss exponent, f is the carrier frequency, c denotes the speed of light; and $\xi_{LoS,\,j}$ and $\xi_{NLoS,\,j}$ are the average environment-dependent excessive path losses in dB [14] corresponding to GN_j. $p_{LoS,\,j}$ in (2) denotes the probability that the UAV has a LoS to GN_j, and is given by [14]

$$p_{LoS,\,j} = \frac{1}{1 + a\exp\left(-b\;\left(\frac{180}{\pi}\theta_j - a\right)\right)}, \tag{5}$$

where a and b are constant values related to the environment, and θ_j is the elevation angle in radian related to node GN_j. We have $\theta_j = \arccos(h_u/d_j)$, where h_u is the altitude of the UAV and d_j is the Euclidean distance between the UAV and GN_j (see Fig. 1). Using (2)–(5), we obtain

$$L_{d,j} = \frac{\xi_{LoS,\,j} - \xi_{NLoS,\,j}}{1 + a\exp\left(-b\;\left(\frac{180}{\pi}\theta_j - a\right)\right)} + 20\log\left(\frac{4\pi f d_j}{c}\right) + \xi_{NLoS,\,j}, \tag{6}$$

where the distance d_j is given by

$$d_j = \sqrt{(X_u - X_j)^2 + (Y_u - Y_j)^2 + (h_u - h_j)^2}, \tag{7}$$

where (X_u, Y_u, h_u) indicates the position of the UAV in sky. The unmodulated transmit signal vector $\mathbf{x}_j(t)$ from the N_u UAV antennas is $\mathbf{x}_j(t) = \Re\{\sqrt{2P_j}\mathbf{w}_j e^{i2\pi f t}\}$, where $\mathbf{w}_j$ is the energy beamforming complex vector with unit norm—assuming availability of perfect channel state information (CSI) on the UAV side—and P_j is the transmit power destined for GN_j. The maximum harvested energy by GN_j from the UAV during τ dedicated for WPT operation is given by

$$E_j = \eta_j P_j |\mathbf{h}_j \mathbf{w}_j^{\star}|^2 \tau = \eta_j P_j \|\mathbf{h}_j\|^2 \tau = \eta_j \frac{P_j}{L_{d,j}} \|\mathbf{h}'_j\|^2 \tau, \tag{8}$$

where $0 < \eta_j \leq 1$ is the energy-harvesting circuit efficiency [15]. The optimal weight vector $\mathbf{w}_j^{\star}$ is equal to $\mathbf{h}_j^{\dagger}/\|\mathbf{h}_j\|$ with $\dagger$ denoting Hermitian transposition; thus leading to the energy expression as in (8).

The ground nodes use the harvested energy for the uplink communication with the BS. Without loss of generality, we assume that the time slot duration T is unity. The received data signal at the BS from node j is given by

$$\mathbf{y}_j = \sqrt{\frac{E_j/L_{b,j}}{1-\tau}}\; \mathbf{g}_j\; s_j + \mathbf{n}_j, \tag{9}$$

where $s \in \mathbb{C}$ is the normalized data symbol with zero mean and unit magnitude, $\mathbf{y}_j \in \mathbb{C}^{N_b \times 1}$, and $\mathbf{n}_j \in \mathbb{C}^{N_b \times 1}$ is the additive Gaussian noise with zero mean and covariance matrix $\mathbb{E}\{\mathbf{n}_j \mathbf{n}_j^\dagger\} = \sigma_j^2 \mathbf{I}_{N_b}$. Further, $\mathbf{g}_j$ denotes the normalized uplink small-scale fading channel vector distributed as $\mathcal{CN} \sim (0, \mathbf{I}_{N_b})$, and $L_{b,j}$ is the distance-dependent path loss of the GN_j-BS link. With perfect CSI at the BS, maximum ratio combining (MRC) is implemented. Assuming that the channel coefficients $\mathbf{h}_j$ and $\mathbf{g}_j$ are constant during each time slot, the transmission rate related to GN_j, considering the OMA scheme, is given by

$$\begin{aligned} R_j(P_j, \tau, d_j, \theta_j) &= \frac{1-\tau}{2} W_j \log_2 \left(1 + \frac{2E_j \|\mathbf{g}_j\|^2 / L_{b,j}}{(1-\tau)\Gamma_j \sigma_j^2}\right) \\ &= \frac{1-\tau}{2} W_j \log_2 \left(1 + \frac{2\eta_j P_j \|\mathbf{h}'_j\|^2 \|\mathbf{g}_j\|^2 \tau}{L_{b,j} L_{d,j} (1-\tau)\Gamma_j \sigma_j^2}\right) \end{aligned} \tag{10}$$

where W_j is the bandwidth related to GN_j, $\Gamma_j > 1$ is the signal-to-noise ratio (SNR) gap to account for the lower performance of physically realizable encoding systems compared to the ideal Shannon-capacity reaching ones. Note that $L_{d,j}$ is itself a function of d_j and θ_j as per (6). The UAV can also adjust its charging power P_j and charging time duration τ.

Exploiting the idea of channel hardening [16], namely that $\lim_{N_b \to \infty} \frac{\|\mathbf{g}_j\|^2}{N_b} = 1$ in large-scale MIMO, (10) becomes

$$R_j(P_j, \tau, d_j, \theta_j) = \frac{1-\tau}{2} W_j \log_2 \left(1 + \frac{2\eta_j P_j \|\mathbf{h}'_j\|^2 N_b \tau}{L_{b,j} L_{d,j} (1-\tau)\Gamma_j \sigma_j^2}\right). \tag{11}$$

By using the Jensen's inequality, we can write

$$\begin{aligned} &\mathbb{E}\left[\frac{1-\tau}{2} W_j \log_2 \left(1 + \frac{2\eta_j P_j \|\mathbf{h}'_j\|^2 N_b \tau}{L_{b,j} L_{d,j} (1-\tau)\Gamma_j \sigma_j^2}\right)\right] \\ &\leq \frac{1-\tau}{2} W_j \log_2 \left(1 + \frac{2\eta_j P_j \mathbb{E}\left[\|\mathbf{h}'_j\|^2\right] N_b \tau}{L_{b,j} L_{d,j} (1-\tau)\Gamma_j \sigma_j^2}\right) \\ &\overset{(a)}{=} \frac{1-\tau}{2} W_j \log_2 \left(1 + \frac{2\eta_j P_j N_b \tau}{L_{b,j} L_{d,j} (1-\tau)\Gamma_j \sigma_j^2}\right), \end{aligned} \tag{12}$$

where (a) in (12) gives an upper-bound for the average transmission rate of GN_j. Let us define the throughput as the sum-rate of the system:

$$R(\mathbf{P}, \tau, \mathbf{d}, \boldsymbol{\theta}) = \sum_{j=1}^{2} R_j(P_j, \tau, d_j, \theta_j). \tag{13}$$

where $\mathbf{P} = [P_1, P_2]$, $\mathbf{d} = [d_1, d_2]$, and $\boldsymbol{\theta} = [\theta_1, \theta_2]$.

III. Energy-Efficient Power Allocation

The energy efficiency of the wireless powered communication system can be evaluated by defining the energy efficiency coefficient

$$\rho_E = \frac{R(\mathbf{P}, \tau, \mathbf{d}, \boldsymbol{\theta})}{P_0 \tau + P\tau}, \tag{14}$$

where P_0 is the constant power consumption of the UAV which significantly includes the electrical power to keep the UAV moving in air, and $P = P_1 + P_2$ is the transmit power. Having assumed spherical coordinates (d_j, θ_j, ϕ_j) and noticing that $L_{d,j}$ does not depend on ϕ_j, we try to solve the below optimization problem to decide first on the optimized position of the UAV in the sky according to the demand parameters, μ_1 and μ_2. Then, optimization of the transmit powers, P_1, P_2, and the harvesting time τ by both nodes is tackled. The problem is formulated as follows:

$$\begin{aligned} \max_{P, \tau, d_j, \theta_j} \quad & \rho_E \\ \text{subject to:} \quad & P_1 + P_2 \leq P_{u,max}, \\ & \frac{E_j}{1-\tau} \leq P_{GN_j,max}, \quad j = 1, 2, \\ & \tau < 1, \\ & r_{j,min} \leq R_j(P_j, \tau, d_j, \theta_j), \quad j = 1, 2, \\ & h_{u,min} \leq d_j \cos(\theta_j), \quad j = 1, 2, \end{aligned} \tag{15}$$

where $P_{GN_j,max}$ and $P_{u,max}$ are the maximum transmit power of GN_j and the UAV, respectively; $r_{j,min}$ denotes the minimum expected transmission rate of node GN_j during each time slot, and $h_{u,min}$ is the minimum allowed height for the UAV. Note that $d_j \cos(\theta_j) = h_u$.

We split the optimization problem into two sub-problems. In the first one (OP1), we aim to find the optimum position of the UAV, i.e., the optimal distances and elevation angles with respect to the GNs according to their demands. In the second problem (OP2), and after getting the optimum position of the UAV, we determine the optimal power and switching time.

A. The UAV Positioning

In OP1, we care about θ_j and d_j which are given in (6) for both nodes at the same time. This can be achieved by connecting the path losses for two A2G channels related to each node by the parameters pertaining to the nodes' demands. So, OP1 will be as follows:

$$\begin{aligned} \text{OP1:} \quad & \min_{d_j, \theta_j} \quad \mu_1 L_{d,1} + \mu_2 L_{d,2} \\ & \text{subject to:} \quad h_{u,min} \leq d_j \cos(\theta_j), \quad j = 1, 2. \end{aligned} \tag{16}$$

This optimization problem can be solved by introducing the vector of Lagrangian multipliers $\boldsymbol{\lambda} = [\lambda_1, \lambda_2]$. The objective function then becomes

$$\begin{aligned} \mathcal{L}_1(\boldsymbol{\lambda}, \mathbf{d}, \boldsymbol{\theta}) = \mu_1 L_{d,1} + \mu_2 L_{d,2} - \lambda_1 h_{u,min} - \lambda_2 h_{u,min} \\ - \lambda_1 d_1 \cos(\theta_1) - \lambda_2 d_2 \cos(\theta_2). \end{aligned} \tag{17}$$

Exploiting the Karush–Kuhn–Tucker (KKT) conditions, one can get the optimal position of the UAV by solving the first derivatives of $\mathcal{L}_1$ with respect to d_j and θ_j, respectively, as follows:

$$\begin{aligned} \frac{\partial \mathcal{L}_1}{\partial d_j} &= \mu_j \frac{\partial L_{d,j}}{\partial d_j} - \lambda_j \\ &= \frac{20\,\mu_j}{d_j \ln(10)} - \lambda_j \cos(\theta_j) \\ &= 0, \quad j \in \{1, 2\}, \end{aligned} \tag{18}$$

$$\begin{aligned}\frac{\partial \mathcal{L}_1}{\partial \theta_j} &= \frac{\partial L_{d,j}}{\partial \theta_j} + \lambda_j d_j \sin(\theta_j)\\ &= \frac{ab\frac{180}{\pi}(\xi_{LoS,\,j} - \xi_{NLoS,\,j}) \exp\left(-b\left(\frac{180}{\pi}\theta_j - a\right)\right)}{\left(1 + a\exp\left(-b\left(\frac{180}{\pi}\theta_j - a\right)\right)\right)^2}\\ &+ \lambda_j d_j \sin(\theta_j)\\ &= 0, \quad j \in \{1,2\}. \end{aligned} \tag{19}$$

The new value of λ_j can be simply calculated using the gradient decent method as follows:

$$\lambda_j(i+1) = [\lambda_j(i) - \triangle_{\lambda_j}(h_{u,min} - d_j\cos(\theta_j))]^+, \tag{20}$$

where $\lambda_j(i)$, $j \in \{1,2\}$, is the value of λ_j at the i^{th} iteration, $\triangle_{\lambda_j}$ is the iteration step, and $[x]^+ = \max(0,x)$. As a starting point, we set $\lambda_j = 0$ for $j \in \{1,2\}$ as mentioned in Algorithm 1 and then update it in each iteration. The output of the optimization will be the optimum position of the UAV, i.e. θ_j^* and d_j^*, corresponding to GN_j, $j \in \{1,2\}$. Algorithm 1 summarizes the procedure for finding the optimal positioning of the UAV. Notice that the position of the GNs are known. The results will be used in the second optimization problem.

Algorithm 1 3D Position Optimization (X_u^*,Y_u^*,h_u^*)

Input: [X_j,Y_j,h_j], μ_j, $\xi_{LoS,\,j}$, $\xi_{NLoS,\,j}$ for $j \in \{1,2\}$; a, b, $h_{u,min}$, f.
Output: [X_u^*,Y_u^*,h_u^*]
Initialization : [X_{u0},Y_{u0},h_{u0}], $\lambda_j = 0$ for $j \in \{1,2\}$.

1: Update λ_j's according to (20).
2: Solve (18) for d_j, $j \in \{1,2\}$.
3: Solve (19) for θ_j, $j \in \{1,2\}$.
4: Compute the optimal [X_u^*,Y_u^*,h_u^*] by solving (16)

B. Energy-Efficient Resource Allocation

In OP2, we eliminate the last constraint in (15) which is already covered by OP1. With the remaining constraints, the optimization problem is formulated as follows:

$$\begin{aligned} \text{OP2:} \quad & \max_{P_1,P_2,\tau} \quad \rho_E\\ & \text{subject to:} \quad P_1 + P_2 \leq P_{u,max},\\ & \qquad \frac{E_j}{1-\tau} \leq P_{GN_j,max}, \quad j = 1,2,\\ & \qquad \tau < 1,\\ & \qquad r_{j,min} \leq R_j(P_j,\tau,d_j^*,\theta_j^*), \quad j = 1,2. \end{aligned} \tag{21}$$

From the first and second constraints in (21), and by substituting (8) in the second constraint in (21); and assuming that both GNs have the same maximum transmit power $P_{GN,max}$ and energy-harvesting efficiency η, we can deduce that $\tau \leq \tau_{max}$, where

$$\tau_{max} = \frac{P_{GN,max} L_{d,1} L_{d,2}}{\eta P_{u,max}(\mu_1 L_{d,2} + \mu_2 L_{d,1}) + L_{d,1} L_{d,2} P_{GN,max}}. \tag{22}$$

It is obvious that the objective function of OP2 is a fractional optimization problem with variables P_1, P_2, and τ, which is generally non-convex. Exploiting the idea in [17], the fractional programming problem is transformed into a convex problem by introducing the variable z^* as the optimal energy efficiency when we have the optimal powers and optimal switching time, P_1^*, P_2^* and τ^*, respectively. Thus, OP2 is now described as

$$\begin{aligned} \text{OP2*:} \quad & \max_{P,\tau} \quad R(\mathbf{P},\tau,\mathbf{d}^*,\boldsymbol{\theta}^*) - z^*(P_0\tau + P\tau)\\ & \text{subject to:} \quad P_1 + P_2 \leq P_{u,max},\\ & \qquad \tau \leq \tau_{max},\\ & \qquad \tau < 1,\\ & \qquad R_j(P_j,\tau,d_j^*,\theta_j^*), \quad j = 1,2, \end{aligned} \tag{23}$$

Basically OP2* can be efficiently proved to be a convex optimization problem by assuring that the second derivatives of $R(\mathbf{P},\tau,\mathbf{d}^*,\boldsymbol{\theta}^*)$ with respect to P_j and τ, are less than zero.

By introducing $\vartheta \geq 0$, $\varsigma \geq 0$, $\varepsilon \geq 0$, $\varphi_1 \geq 0$, and $\varphi_2 \geq 0$ as the Lagrange multipliers associated with the four constraints in OP2*, respectively, the Lagrangian function of OP2* can be formulated as

$$\begin{aligned} &\mathcal{L}_2(\vartheta,\varsigma,\varepsilon,\varphi_1,\varphi_2,P_1,P_2,\tau) =\\ &\quad R_1(P_1,\tau,d_1^*,\theta_1^*) + R_2(P_2,\tau,d_2^*,\theta_2^*)\\ &\quad - z^*(P_0\tau + P\tau) - \vartheta(P_1+P_2) + \vartheta P_{u,max}\\ &\quad - \varsigma\tau + \varsigma\tau_{max} - \varepsilon\tau + \varepsilon - \varphi_1 r_{1,min} - \varphi_2 r_{2,min}\\ &\quad + \varphi_1 R_1(P_1,\tau,d_1^*,\theta_1^*) + \varphi_2 R_2(P_2,\tau,d_2^*,\theta_2^*). \end{aligned} \tag{24}$$

To find the optimal transmit powers P_1^* and P_2^* from the UAV towards GN_1 and GN_2, respectively, we assume that the UAV will use its maximum power during the WPT period, which simply means that $P_2^* = P_{u,max} - P_1^*$. Our aim now is to get P_1^* which also implicitly means P_2^* and the optimal WPT time τ^*. Taking into consideration that OP2* is a nonlinear programming problem, this can be done through derivation of the Lagrangian function with respect to P_1 and τ, respectively, as follows:

$$\begin{aligned} &\frac{\partial \mathcal{L}_2(\vartheta,\varsigma,\varepsilon,\varphi_1,\varphi_2,P_1,\tau)}{\partial P_1}\\ &= (1+\varphi_1)\frac{\partial R_1(P_1,\tau,d_1^*,\theta_1^*)}{\partial P_1} + (1+\varphi_2)\frac{\partial R_2(P_1,\tau,d_2^*,\theta_2^*)}{\partial P_1}\\ &- z^*\tau - \vartheta\\ &= \frac{(1+\varphi_1)(1-\tau)W_1}{2P_1\ln 2} - \frac{(1+\varphi_2)(1-\tau)W_2 P_1}{2(P_{u,max}-P_1)\ln 2}\\ &- z^*\tau - \vartheta\\ &= 0, \end{aligned} \tag{25}$$

$$\begin{aligned} &\frac{\partial \mathcal{L}_2(\vartheta,\varsigma,\varepsilon,\varphi_1,\varphi_2,P_1,\tau)}{\partial \tau}\\ &= (1+\varphi_1)\frac{\partial R_1(P_1,\tau,d_1^*,\theta_1^*)}{\partial \tau} + (1+\varphi_2)\frac{\partial R_2(P_1,\tau,d_2^*,\theta_2^*)}{\partial \tau}\\ &- z^* P_{u,max} - z^* P_0 - \varsigma - \varepsilon\\ &= \frac{(1+\varphi_1)W_1}{2}\left(\frac{(1-\tau)}{\tau\ln 2} - \log_2\left(\frac{\eta_1 P_1 N_b \tau}{L_{b,1}L_{d,1}(1-\tau)\Gamma_1\sigma_1^2}\right)\right)\\ &+ \frac{(1+\varphi_2)W_2}{2}\left(\frac{(1-\tau)}{\tau\ln 2} - \log_2\left(\frac{\eta_2(P_{u,max}-P_1)N_b\tau}{L_{b,2}L_{d,2}(1-\tau)\Gamma_2\sigma_2^2}\right)\right)\\ &- z^* P_{u,max} - z^* P_0 - \varsigma - \varepsilon\\ &= 0. \end{aligned} \tag{26}$$

The updating of the Lagrangian variables ϑ, ς , ε, φ_1 and φ_2 can be done using the gradient method as follows:

$$\vartheta(i+1) = [\vartheta(i) - \triangle_{\vartheta}(P_{u,max} - P)]^{+} \tag{27}$$

$$\varsigma(i+1) = [\varsigma(i) - \triangle_{\varsigma}(\tau_{max} - \tau)]^{+} \tag{28}$$

$$\varepsilon(i+1) = [\varepsilon(i) - \triangle_{\varepsilon}(1 - \tau)]^{+} \tag{29}$$

$$\varphi_1(i+1) = [\varphi_1(i) - \triangle_{\varphi_1}(R_1(P_1, \tau, \theta_1^*, d_1^*) - r_{1,min})]^{+} \tag{30}$$

$$\varphi_2(i+1) = [\varphi_2(i) - \triangle_{\varphi_2}(R_2(P_1, \tau, \theta_2^*, d_2^*) - r_{2,min})]^{+}, \tag{31}$$

where i is the iteration index, and the $\triangle_{\vartheta}$, $\triangle_{\varsigma}$, $\triangle_{\varepsilon}$, $\triangle_{\varphi_1}$, and $\triangle_{\varphi_2}$ are the iteration steps.

The solution of OP2, by depending on the expressions (21)–(31) and the output of Algorithm 1, is summarized in Algorithm 2.

Algorithm 2 Energy-Efficient Resource Allocation

Input: Output of Algorithm (1) $[X_u^*, Y_u^*, h_u^*]$, $[X_1, Y_1, h_1]$, $[X_2, Y_2, h_2]$, $[X_b, Y_b, h_b]$, $h_{u,min}$, a, b, $\xi_{LoS,j}$, $\xi_{NLoS,j}$, f, N_u, N_b, $L_{d,j}$, $L_{b,j}$, η_j, Γ_j, σ_j, $r_{1,min}$, $r_{2,min}$, $\triangle_{\vartheta}$,$\triangle_{\varsigma}$, $\triangle_{\varepsilon}$, $\triangle_{\varphi_1}$, $\triangle_{\varphi_2}$, and z^*.

Output: $[P_1^*, P_2^*, \tau^*]$.

Initialization: $[P_{1_0}, \tau_0]$, $\vartheta = 0$, $\varsigma = 0$, $\varepsilon = 0$, $\varphi_1 = 0$, $\varphi_2 = 0$.

1: Update ϑ, ς , ε, φ_1, and φ_2 based on (27), (28), (29), (30), and (31), respectively.

2: Solve (25) and (26) jointly to obtain P_1 and τ.

3: Compute the optimal $[P_1^*, P_2^*, \tau^*]$ by solving (23).

IV. Numerical Results

In the simulations, we assume the propagation parameters to correspond to an urban environment [14], unless stated otherwise. We choose $a = 9.6$, $b = 0.28$, $\xi_{LoS,j} = 1$ dB, $\xi_{NLoS,j} = 20$ dB, $f = 2$ GHz, $\Gamma_j = 1.2$, $W_j = 200$ kHz, $\eta_j = 0.8$, $\sigma_j^2 = 1$; for $j = 1, 2$. The coordinates of GN_1, GN_2 and the BS are set to [500 0 0], [-500 0 0] and [0 100 25], respectively. The UAV position is the output of OP1 with $h_{u,min} = 100$ m. Moreover, we set $P_0 = 10$ Watt, $P_{u,max} = 3$ Watt, $N_u = 5$ and $N_b = 100$, unless stated otherwise.

A. 3D Position of the UAV

The proposed algorithm for finding the optimal 3D position of the UAV, i.e., Algorithm 1, efficiently converges to the optimal position with respect to d_j and θ_j where $j = 1, 2$, after no more than 10 iterations for different initial settings. Afterwards, this output is used in OP2.

With two GNs, we have three cases: (i) the demand of GN_1 is larger than the demand of GN_2, i.e., $\mu_1 > \mu_2$; (ii) the demand of GN_2 is larger than that of GN_1, i.e., $\mu_2 > \mu_1$; and (iii) both have the same demand, i.e., $\mu_1 = \mu_2$. These three cases are clearly illustrated in Fig. 2, which represents the optimal horizontal location of the UAV depending on the values of μ_1 and μ_2. For instance, when $\mu_1 = 0.8$ and $\mu_2 = 0.2$, the UAV hovers at the position of [300 0 100]. In the extreme case where the demand of one GN is at most whereas the other has no demand, the path loss will be on its minimum with respect to the former node and to the maximum with respect to the latter. For example, when GN_1 has maximum demand, $\mu_1 = 1$, then the UAV will hover directly on top of it, i.e. at the position [500 0 100]. In the case of same demands, where $\mu_1 = \mu_2 = 0.5$, the path losses will be the same for both nodes and the UAV will be at the medium point [0 0 100] between the nodes.

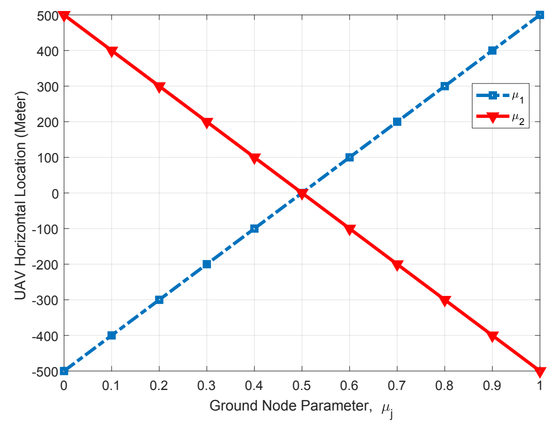

Fig. 2. UAV position according to the nodes' demands.

B. Energy Efficiency with Optimal Power and Charging Time

Figure 3 shows the transmit powers from the UAV towards the GNs, as a function of the demand parameter of GN_1, i.e., μ_1. The figure compares P_1^* and P_2^* when the UAV takes the demand parameters of the GNs into consideration and when not. It is clear that the UAV transmit power will be divided equally among the GNs and that the UAV will hover in the middle between them when demand parameters are not taken into account. For instance, when $\mu_1 = 0.7$ and the UAV takes the GN demands into account, a power of $P_1^* = 2.45$ Watt and $P_2^* = 1.35$ Watt will be allocated towards GN_1 and GN_2, respectively. On the other hand, when the UAV does not take the demands into consideration,the power levels will be fixed to 1.5 Watt regardless of the nodes' requirements for the data communication on the uplink.

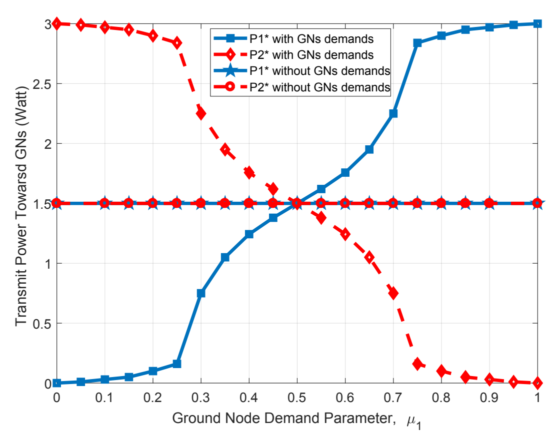

Fig. 3. Transmit power towards GNs versus demand parameter of GN_1.

Figure 4 shows the optimal normalized harvesting time, τ^*/T, for different demand values, which also means for the different optimized positions of the UAV. The results are plotted as a function of μ_1, while recalling that the demands are normalized such such that $\mu_1 + \mu_2 = 1$. The figure illustrates the usefulness of optimizing the UAV position according to the GNs' demands. It is clear that in all cases, except when the GNs have equal demands, the WPT time will be lower when the UAV takes the GNs' demands into consideration. For example, when $\mu_1 = 0.8$, i.e., $\mu_2 = 0.2$, the normalized harvesting time is almost 0.3 while it is around 0.6 when GNs' demands are not taken into account. With the ensuing time savings, the UAV can be used for other missions.

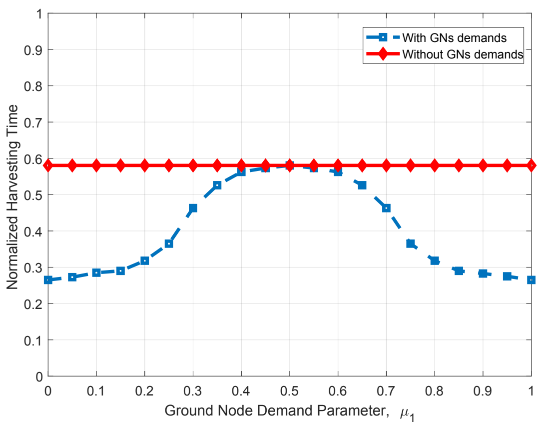

Fig. 4. Normalized harvesting time versus demand parameter of GN_1.

Figure 5 displays the effect of varying demands on the energy efficiency of the system. Similar to Fig. 4, results are plotted as a function of μ_1. The energy efficiency, when the optimization of the UAV position does not take into account the GNs' demands will be fixed. The energy efficiency with optimized UAV position based on the GNs' demands will be better in all cases. Obviously, the result is the same when the GNs have the same demand. For instance, when $N_b = 100$ and $\mu_1 = 0.75$, there is a considerable difference in the energy efficiency when GNs' demands are taken into account and when not. Note that by increasing the number of antennas of the BS, the energy efficiency increases in all cases.

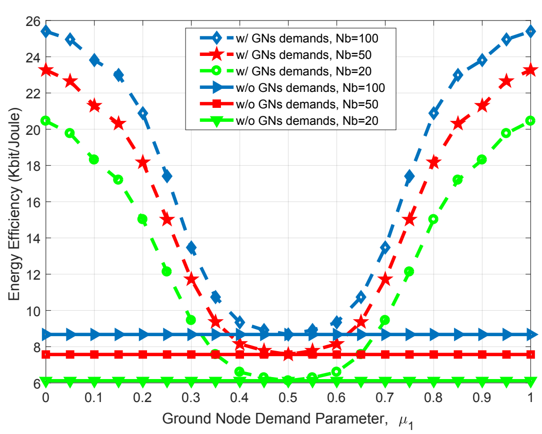

Fig. 5. Energy efficiency versus demand parameter of GN_1.

V. Conclusion

In this work, we have studied the resource allocation problem in a wireless system where a multiple-antenna UAV is deployed for charging ground nodes through RF wireless power transfer so as to assist their uplink data communication with a terrestrial base station. The optimization problem was solved by exploiting the movement flexibility of the UAV, which allows minimizing the path loss on the air-to-ground channels according the nodes' demands, and optimizing the transmit powers towards maximization of the energy efficiency of the system. The results show that significant energy efficiency can be achieved by the proposed allocation scheme. In particular, the results show that less wireless power transfer time will be needed from the UAV to simultaneously charge GNs when their demands are taken into account. Current investigations include operation of the system with non-orthogonal multiple access (NOMA) and comparisons with the OMA scenario.

References

[1] A. Merwaday and I. Guvenc, "UAV assisted heterogeneous networks for public safety communications," in *IEEE Wireless Communications and Networking Conference Workshops*, 2015, pp. 329–334.

[2] C. F. Liew, D. DeLatte, N. Takeishi, and T. Yairi, "Recent developments in aerial robotics: A survey and prototypes overview," *CoRR*, vol. abs/1711.10085, 2017.

[3] J. G. Andrews, S. Buzzi, W. Choi, S. V. Hanly, A. Lozano, A. C. K. Soong, and J. C. Zhang, "What will 5G be?" *IEEE J. Sel. Areas Commun.*, vol. 32, no. 6, pp. 1065–1082, Jun. 2014.

[4] Y. Li, Z. Yuan, and C. Peng, "A control-plane perspective on reducing data access latency in LTE networks," in *ACM Annual International Conference on Mobile Computing and Networking*, 2017, pp. 56–69.

[5] M. Mozaffari, W. Saad, M. Bennis, and M. Debbah, "Unmanned aerial vehicle with underlaid device-to-device communications: Performance and tradeoffs," *IEEE Trans. Wireless Commun.*, vol. 15, no. 6, pp. 3949–3963, Jun. 2016.

[6] L. Sboui, H. Ghazzai, Z. Rezki, and M. S. Alouini, "Energy-efficient power allocation for UAV cognitive radio systems," in *IEEE Vehicular Technology Conference*, 2017, pp. 1–5.

[7] J. Xu, Y. Zeng, and R. Zhang, "UAV-enabled wireless power transfer: Trajectory design and energy optimization," *IEEE Trans. Wireless Commun.*, vol. 17, no. 8, pp. 5092–5106, Aug. 2018.

[8] Y. Zeng, R. Zhang, and T. J. Lim, "Throughput maximization for UAV-enabled mobile relaying systems," *IEEE Trans. Commun.*, vol. 64, no. 12, pp. 4983–4996, Dec. 2016.

[9] M. Alzenad, A. El-Keyi, F. Lagum, and H. Yanikomeroglu, "3-D placement of an unmanned aerial vehicle base station (UAV-BS) for energy-efficient maximal coverage," *IEEE Wireless Commun. Lett.*, vol. 6, no. 4, pp. 434–437, Aug. 2017.

[10] H. Wang, J. Wang, G. Ding, L. Wang, T. A. Tsiftsis, and P. K. Sharma, "Resource allocation for energy harvesting-powered D2D communication underlaying UAV-assisted networks," *IEEE Trans. Green Commun. and Netw.*, vol. 2, no. 1, pp. 14–24, Mar. 2018.

[11] X. Chen, X. Wang, and X. Chen, "Energy-efficient optimization for wireless information and power transfer in large-scale MIMO systems employing energy beamforming," *IEEE Wireless Commun. Lett.*, vol. 2, no. 6, pp. 667–670, Dec. 2013.

[12] R. Narasimhan, "Finite-SNR diversity—multiplexing tradeoff for correlated Rayleigh and Rician MIMO channels," *IEEE Trans. Inf. Theory*, vol. 52, no. 9, pp. 3965–3979, Sep. 2006.

[13] A. Paulraj, R. Nabar, and D. Gore, *Introduction to Space-Time Wireless Communications*. Cambridge University Press, 2003.

[14] A. Al-Hourani, S. Kandeepan, and S. Lardner, "Optimal LAP altitude for maximum coverage," *IEEE Wireless Commun. Lett.*, vol. 3, no. 6, pp. 569–572, Dec. 2014.

[15] M. Xia and S. Aissa, "On the efficiency of far-field wireless power transfer," *IEEE Trans. Signal Process.*, vol. 63, no. 11, pp. 2835–2847, Jun. 2015.

[16] B. M. Hochwald, T. L. Marzetta, and V. Tarokh, "Multiple-antenna channel hardening and its implications for rate feedback and scheduling," *IEEE Trans. Inf. Theory*, vol. 50, no. 9, pp. 1893–1909, Sep. 2004.

[17] D. W. K. Ng, E. S. Lo, and R. Schober, "Energy-efficient resource allocation for secure OFDMA systems," *IEEE Trans. Veh. Technol.*, vol. 61, no. 6, pp. 2572–2585, Jul. 2012.